



# Kent Academic Repository

**Wang, Dayang, Wang, Lijuan and Yan, Yong (2025) *Measurement of Weight Fraction in HDPE Bales Using a Capacitive Sensor and a Weighing Device*. IEEE Transactions on Instrumentation and Measurement, 74 . ISSN 0018-9456.**

## Downloaded from

<https://kar.kent.ac.uk/111978/> The University of Kent's Academic Repository KAR

## The version of record is available from

<https://doi.org/10.1109/TIM.2025.3638012>

## This document version

Publisher pdf

## DOI for this version

## Licence for this version

CC BY (Attribution)

## Additional information

## Versions of research works

### Versions of Record

If this version is the version of record, it is the same as the published version available on the publisher's web site. Cite as the published version.

### Author Accepted Manuscripts

If this document is identified as the Author Accepted Manuscript it is the version after peer review but before type setting, copy editing or publisher branding. Cite as Surname, Initial. (Year) 'Title of article'. To be published in **Title of Journal** , Volume and issue numbers [peer-reviewed accepted version]. Available at: DOI or URL (Accessed: date).

## Enquiries

If you have questions about this document contact [ResearchSupport@kent.ac.uk](mailto:ResearchSupport@kent.ac.uk). Please include the URL of the record in KAR. If you believe that your, or a third party's rights have been compromised through this document please see our [Take Down policy](https://www.kent.ac.uk/guides/kar-the-kent-academic-repository#policies) (available from <https://www.kent.ac.uk/guides/kar-the-kent-academic-repository#policies>).

# Measurement of Weight Fraction in HDPE Bales Using a Capacitive Sensor and a Weighing Device

Dayang Wang<sup>ID</sup>, Lijuan Wang<sup>ID</sup>, *Senior Member, IEEE*, and Yong Yan<sup>ID</sup>, *Fellow, IEEE*

**Abstract**—Weight fraction is a key indicator to classify high-density polyethylene (HDPE) bales with or without contamination into different quality categories, which determine the values of the bales for reuse purpose. However, the main existing technique, sampling and testing, is still not able to achieve accurate and efficient measurement of weight fraction in HDPE bales. In this study, a new method combining a capacitive sensor and a weighing device is proposed for the first time to measure the weight fractions of HDPE and a single-known contaminant in HDPE bales, independent of packing density. The purpose-built capacitive sensor, consisting of two pairs of transceiver units, senses the mixture permittivity of the bale from different directions, while the weighing device provides the information of the mixture density of the bale. A mathematical model is established to derive the weight fractions of HDPE and the contaminant based on the mixture permittivity and density obtained from the capacitive sensor and the weighing device. To verify the proposed measurement method, experimental tests were conducted in the laboratory with small-scale model bales. The HDPE bales were mixed with the contaminant, polyvinyl chloride (PVC), and produced with the HDPE weight fraction ranging from 18.0% to 100% and PVC weight fraction ranging from 33.6% to 100%. Experimental results demonstrate that the relative errors of the measured weight fractions of HDPE and the contaminant are within  $\pm 5\%$  under laboratory conditions.

**Index Terms**—Capacitive sensor, high-density polyethylene (HDPE) bale, polyvinyl chloride (PVC), weighing method, weight fraction.

## I. INTRODUCTION

HIGH-DENSITY polyethylene (HDPE) is a type of commonly used plastic and also a relatively sustainable material due to the fact that it is widely recycled and usually undergoes closed-loop recycling. However, its sustainability is significantly affected by the quality of HDPE bales during the recycling process. The total HDPE fraction by weight is a key indicator to define the grade of a bale [1]. Due to a series of sorting processes in material recovery facility before baling, HDPE bales usually don't contain a large variety of contaminants, and an HDPE bale containing a single

contaminant is one of the encountered scenarios. The presence of the contaminant would lower the bale's grade, making it difficult to recycle and resulting in low-value products. In general, the industry-developed guidelines for recycling market require that the total contamination should not exceed 15% by weight, and the individual allowable contaminants should not exceed 5% [2]. Exceeding the specified limit may reduce bale value. Therefore, accurate and efficient measurement of weight fraction in HDPE bales is important not only for quality control of recycled HDPE but also to improve the efficiency of the recycling process and enhance the sustainability of HDPE.

Currently, the recycling industry primarily relies on sampling and testing to assess the composition of recyclates and detect the presence of contaminants in bales. In addition, each bale is required to be visually inspected on five sides for contamination and odors that may indicate contamination [3]. Even though the guidance for sampling and testing has been developed for material facilities to ensure an appropriate sampling [4], it is still time-consuming and the measurement accuracy is uncertain due to many manual operations involved. Development of an accurate, efficient, and low-cost measurement system for automatically quantifying weight fraction in HDPE bales is highly demanded. However, there is currently a lack of research in this area.

A number of methods have been investigated for material sorting, including ultrasound method [5], microwave method [6], X-ray method [7], near-infrared spectroscopy [8], [9], hyperspectral imaging [10], [11], and capacitive method [12], [13], [14]. However, these methods are only designed for sorting separated materials rather than baled materials, let alone measuring the weight fraction. Furthermore, these methods exhibit various limitations if they are applied to measuring the fractions of baled materials. The ultrasound method is affected by various factors that influence its acoustic characteristics and reflection properties. The microwave method often involves high costs and poses difficulties in hardware development. The X-ray method is regarded as environmentally hazardous due to radiation safety concerns, high-energy consumption, substantial capital costs, and administrative challenges. Although the near-infrared spectroscopy and hyperspectral imaging offer an accurate way for identification of different types of plastics by analyzing the spectral information across near-infrared range, both of them typically require costly equipment and have difficulties to detect the materials inside the bale due to their limited penetration depth. Capacitive sensing offers the advantages of rapid response, low cost, and design flexibility,

Received 25 September 2025; revised 3 November 2025; accepted 7 November 2025. Date of publication 27 November 2025; date of current version 9 December 2025. This work was supported by the Engineering and Physical Sciences Research Council under Grant EP/W026228/1. The Associate Editor coordinating the review process was Dr. Yifan Li. (Corresponding author: Lijuan Wang.)

Dayang Wang and Lijuan Wang are with the School of Engineering, Mathematics and Physics, University of Kent, CT2 7NT Canterbury, U.K. (e-mail: dw523@kent.ac.uk; l.wang@kent.ac.uk).

Yong Yan is with Hangzhou International Innovation Institute, Beihang University, Hangzhou 311115, China (e-mail: yongyan@buaa.edu.cn).

Digital Object Identifier 10.1109/TIM.2025.3638012

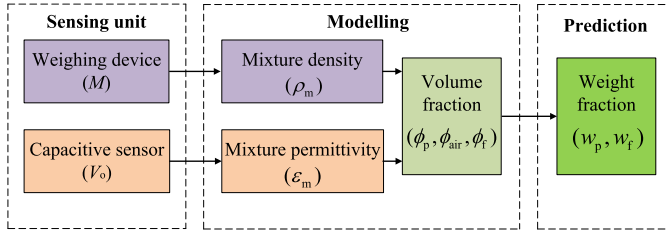


Fig. 1. Principle of weight fraction measurement.

enabling the design of sensor structures suitable for various applications, such as mass flow measurement [15], concentration measurement [16], [17], [18], water fraction measurement [19], water film measurement [20], and tomographic imaging [21], [22], [23], [24], [25]. Our previous study has demonstrated the capability of the newly designed capacitive sensor with two measurement channels incorporating a support vector machine to identify the baled materials [26]. However, the composition of materials in each bale is not quantified. Considering the fact that the packing density may vary in the baling process, it is more challenging to determine the weight fraction.

This article addresses the scenario of HDPE bales containing a single-known contaminant with varying packing density, and presents a new method for measuring the weight fraction in HDPE bales by combining a purpose-built capacitive sensor with a weighing device, which is independent of packing density. The design of the capacitive sensor and corresponding ac-based capacitance measuring circuit is specifically described. A mathematical model is proposed to determine the weight fractions of HDPE and the contaminant in the HDPE bale from the outputs of the capacitive sensor and the weighing device. In addition, experimental work was undertaken in laboratory to measure the weight fraction of the model HDPE bales. The measurement methodology is explained step by step, and the measurement results including sensor outputs and measured weight fractions are analyzed and discussed as well.

## II. METHODOLOGY

### A. Measurement Principle

The principle of weight fraction measurement using a capacitive sensor and a weighing device is shown in Fig. 1. In this study, the proposed method focuses on measuring HDPE bales containing a known contaminant while addressing the impact of uncertainty in packing density on weight fraction measurements. An HDPE bale can thus be considered as consisting of three components: HDPE, the contaminant, and air. The volume fraction of air reflects the packing density. Our goal is to predict the weight fraction  $w_p$  of the HDPE and the weight fraction  $w_f$  of the contaminant. The weight fractions are related to the information of density, permittivity, and volume fraction. Therefore, the sensing unit and the modeling part are designed to obtain these parameters and establish their mathematical relationships. The sensing unit includes a weighing device and a capacitive sensor. The weighing device measures the total mass  $M$  of the HDPE bale which directly

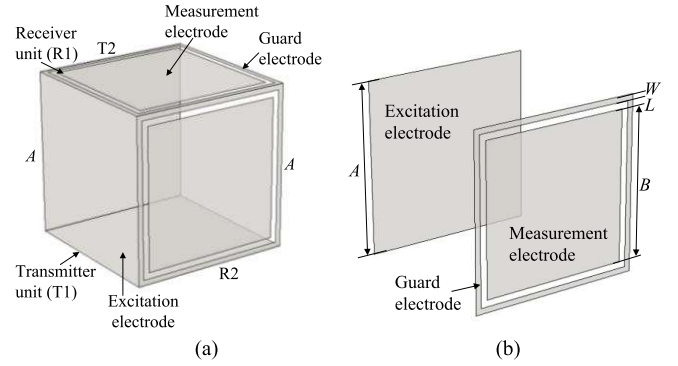


Fig. 2. (a) Structure of the capacitive sensor. (b) Details of the front of the receiver unit.

reflects its mixture density  $\rho_m$ . The output  $V_o$  of capacitive sensor closely relates to the mixture permittivity  $\epsilon_m$  of the bale. To determine the mixture density and permittivity from the outputs of the weighing device and the capacitive sensor, the relationships between mixture density and total mass, as well as between mixture permittivity and voltage output, should be experimentally quantified and established as prior knowledge. Given a bale to be tested, this prior knowledge will be used to calculate its mixture density and mixture permittivity, which are needed in the following mathematical model. The purpose of the modeling part is to establish the mathematical model that utilizes the mixture density and permittivity information obtained from the sensing unit to derive the volume fractions  $\phi_p$ ,  $\phi_{air}$ , and  $\phi_f$  of HDPE, air, and the contaminant in the bale. A detailed introduction will be provided in the mathematical modeling section. Then based on the measured mixture density and the volume fractions, the weight fraction  $w_p$  of the HDPE and the weight fraction  $w_f$  of the contaminant can be calculated.

### B. Capacitive Sensor Design

In this study, a commercial electronic scale is used as the weighing device. The capacitive sensor and the associated hardware circuit are specifically designed and optimized. The structure of the capacitive sensor is shown in Fig. 2(a). The capacitive sensor has four square units including two identical transmitter units (T1 and T2) and two identical receiver units (R1 and R2). A transmitter unit and a receiver unit opposite to each other and form a measurement channel; therefore, the sensor has two measurement channels which measure the bale from two different directions. The transmitter and the receiver units have a length of  $A$  and a thickness of  $t$ , with the ground planes located on their backside. The excitation electrode, the guard electrode, and the measurement electrode are located on the front side of the units. For the transmitter unit, the excitation electrode with the length  $A$  is positioned on the front side of the transmitter unit. For the receiver unit, the measurement electrode with length of  $B$  and a guard electrode with wide of  $W$  are positioned on the front of the receiver unit. The details of the front of the receiver unit are shown in Fig. 2(b). The guard electrode arranged around the measurement electrode is used to reduce

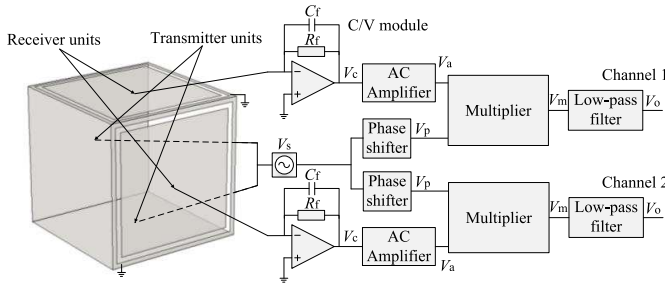


Fig. 3. Circuit diagram of capacitive sensor system.

the fringe field effect. The length between the measurement electrode and the guard electrode is  $L$ . The optimal values of  $A, B, W$ , and  $L$  are determined by considering the size the bale under test and achieving higher sensitivity and more uniform sensitivity distribution through finite element method. The detailed optimization process has been explained in our previous study [26].

An ac-based capacitance measuring circuit with the characteristics of high-resolution and high signal-to-noise ratio [23], [27], [28] is designed for the capacitive sensor. Fig. 3 shows the circuit diagram of the capacitive sensor system. A sinusoidal signal,  $V_s$ , with a peak-to-peak voltage of 8 V and a frequency of 200 kHz, is applied to the excitation electrodes, while the measurement electrodes are connected to the capacitance-to-voltage (C/V) modules. In the C/V module,  $C_f$  and  $R_f$  are set to 2 pF and 51 k $\Omega$ , respectively, to ensure effective conversion of the capacitance signal into a voltage signal. The output voltage  $V_c$  after the C/V module is amplified by the amplifier, and the output signal  $V_a$  is fed into a multiplier. The signal  $V_s$  is applied to a phase shifter to adjust its phase to align with the phase of  $V_a$ , producing the signal  $V_p$ . The multiplier multiplies the two signals to obtain  $V_m$ , and a low-pass filter is designed to eliminate high-frequency part of the  $V_m$ , and the remain part  $V_o$  is related to the measured capacitance  $C_m$ . Since  $C_m$  depends on the mixture permittivity  $\epsilon_m$  of the bale, the voltage output  $V_o$  of the capacitive sensor has a relationship with the mixture permittivity  $\epsilon_m$ . Finally, the designed capacitive sensor system is used together with a commercial weighing device to form a combined sensor system for measuring the HDPE bales.

### C. Mathematical Modeling

For an HDPE bale consisting of three components: HDPE, the contaminant and air, the weight fraction of an individual component is defined as the mass of the component divided by the total mass of the bale  $M$ . Hence, for the HDPE with a mass of  $M_p$ , its weight fraction  $w_p$  is defined as

$$w_p = \frac{M_p}{M} = \frac{\phi_p \rho_p}{\rho_m} \quad (1)$$

where  $\phi_p$  and  $\rho_p$  are volume fraction and density of HDPE, respectively, and  $\rho_m$  is the mixture density of the bale.

The weight fraction  $w_f$  of the contaminant is defined as

$$w_f = \frac{M_f}{M} = \frac{\phi_f \rho_f}{\rho_m} \quad (2)$$

where  $\phi_f$  and  $\rho_f$  are volume fraction and density of the contaminant, respectively.

As the sum of volume fractions of HDPE  $\phi_p$ , the contaminant  $\phi_f$ , and air  $\phi_{air}$  is equal to 1

$$\phi_p + \phi_f + \phi_{air} = 1. \quad (3)$$

The weight fraction  $w_f$  in (2) can be expressed as

$$w_f = \frac{(1 - \phi_p - \phi_{air}) \rho_f}{\rho_m}. \quad (4)$$

The density of HDPE  $\rho_p$  and density of the contaminant  $\rho_f$  are usually known constants, and the mixture density  $\rho_m$  can be determined from the total  $M$  by the weighing device in practice. In this case, the HDPE weight fraction  $w_p$  is purely dependent on its volume fraction  $\phi_p$ , and the weight fraction  $w_f$  is determined by the volume fraction  $\phi_p$  and  $\phi_{air}$ . The problem of determination of weight fractions  $w_p$  and  $w_f$  is now converted to exploring the volume fractions  $\phi_p$  and  $\phi_{air}$ .

The mixture density  $\rho_m$  of a bale can be represented by using the density and volume fraction of individual components within the bale and defined as

$$\rho_m = \rho_p \phi_p + \rho_f \phi_f + \rho_{air} \phi_{air} \quad (5)$$

where  $\rho_{air}$  is the density of the air.

According to (3), (5) can be rewritten as

$$\rho_m = \rho_p \phi_p + \rho_f (1 - \phi_p - \phi_{air}) + \rho_{air} \phi_{air}. \quad (6)$$

Rearrange (6),  $\phi_p$  is a function of  $\rho_m, \rho_p, \rho_f, \rho_{air}$ , and  $\phi_{air}$

$$\phi_p = \frac{-\rho_m - (\rho_f - \rho_{air}) \phi_{air} + \rho_f}{\rho_p - \rho_p} = f(\phi_{air}). \quad (7)$$

In (7), the  $\rho_f, \rho_p$ , and  $\rho_{air}$  are known constants, and  $\phi_p$  is a function of mixture density  $\rho_m$  and  $\phi_{air}$ . The mixture density  $\rho_m$  can be deduced from the weighing device in practice, but  $\phi_p$  still cannot be obtained if  $\phi_{air}$  is unknown.

The mixture permittivity  $\epsilon_m$  of a bale can be represented with the permittivity and volume fraction of individual components and defined as

$$\epsilon_m = \epsilon_p \phi_p + \epsilon_f \phi_f + \epsilon_{air} \phi_{air} \quad (8)$$

where  $\epsilon_p, \epsilon_f, \epsilon_{air}$ , are permittivity of HDPE, the contaminant and air, respectively.

According to (3), (8) can be rewritten as

$$\epsilon_m = \epsilon_p \phi_p + \epsilon_f (1 - \phi_p - \phi_{air}) + \epsilon_{air} \phi_{air}. \quad (9)$$

Rearrange (9),  $\phi_p$  can be represented as a function of  $\epsilon_m, \epsilon_p, \epsilon_f, \epsilon_{air}$ , and  $\phi_{air}$

$$\phi_p = \frac{-\epsilon_m - (\epsilon_f - \epsilon_{air}) \phi_{air} + \epsilon_f}{\epsilon_p - \epsilon_p} = g(\phi_{air}). \quad (10)$$

In (10), the  $\epsilon_p, \epsilon_f$ , and  $\epsilon_{air}$  are known constants, and  $\phi_p$  is a function of mixture permittivity  $\epsilon_m$  and  $\phi_{air}$ . The mixture permittivity  $\epsilon_m$  can be deduced from the capacitive sensor in practice, but  $\phi_p$  still cannot be obtained if  $\phi_{air}$  is unknown.

By using both (7) and (10) and solving them, the two unknowns  $\phi_{air}$  and  $\phi_p$  can be obtained. Since the weighing device and the capacitive sensor measure the same bale, if the



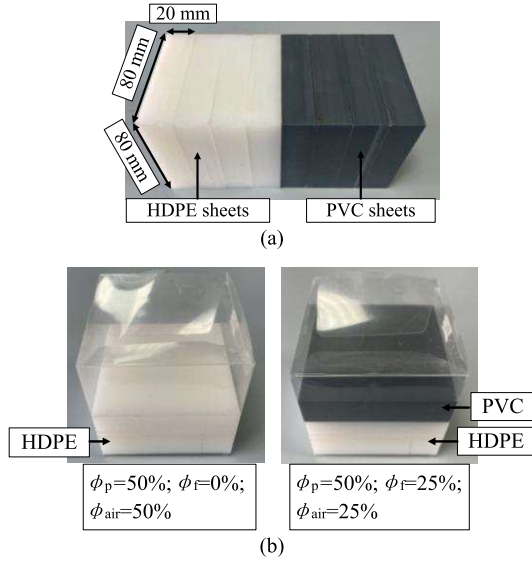


Fig. 4. (a) HDPE sheets and PVC sheets. (b) Bales formed by different plastic sheets with different volume fractions.

TABLE I  
DENSITY AND PERMITTIVITY OF THE EXPERIMENTAL MATERIALS

Materials	Density (g/cm <sup>3</sup> )	Permittivity
HDPE	0.95	2.4
PVC	1.45	3
Air	0.001	1

$\phi_{air}$  is truly determined, the  $\phi_p$  calculated using (7) and (10) should be the same, and their difference should be minimal. Based on this, this study proposes an effective and universal solution method, which minimizes the difference between the two functions  $f(\phi_{air})$  and  $g(\phi_{air})$  in (7) and (10) by finding optimal  $\phi_{air}$

$$\min |f(\phi_{air}) - g(\phi_{air})| \quad \text{s.t. } 0\% \leq \phi_{air} \leq 100\%. \quad (11)$$

Compared with directly solving the equations, this method reduces the uncertainties introduced during the determination of  $\rho_m$  and  $\epsilon_m$  through experimental study and data fitting. Once the optimal  $\phi_{air}$  is determined, the true  $\phi_{air}$  is determined, and the  $\phi_p$  can be calculated by using (7). The corresponding weight fractions  $w_p$  and  $w_f$  can be determined by using (1)–(4), respectively.

### III. EXPERIMENT TESTS

In this study, polyvinyl chloride (PVC), a common plastic, is introduced as a contaminant in HDPE bales to evaluate the ability of the proposed method to determine the weight fractions when the packing density is unknown. During experimental tests, the density and permittivity values of HDPE sheet, PVC sheet, and air used in this study are summarized in Table I. As shown in Fig. 4(a), each HDPE or PVC plastic sheet has dimensions of 80 mm in length, 80 mm in width, and 20 mm in height. By filling different plastic sheets with different numbers into a thin-walled plastic boxes with side length of 80 mm, the bales with different volume fractions and

TABLE II  
BALES USED TO INVESTIGATE SENSOR OUTPUTS AND ESTABLISH PRIOR KNOWLEDGE

Bales	Volume fraction of HDPE (%)	Volume fraction of PVC (%)	Volume fraction of air (%)	Mixture density (g/cm <sup>3</sup> )	Mixture permittivity
1	25	0	75	0.238	1.35
2	50	0	50	0.476	1.7
3	0	50	50	0.726	2
4	50	25	25	0.838	2.2
5	0	75	25	1.088	2.5
6	50	50	0	1.2	2.7
7	0	100	0	1.45	3

TABLE III  
BALES USED FOR EVALUATING THE PERFORMANCE OF THE PROPOSED METHOD

Bales	Volume fraction of HDPE (%)	Volume fraction of PVC (%)	Volume fraction of air (%)	Weight fraction of HDPE (%)	Weight fraction of PVC (%)
1	100	0	0	100	0
2	75	25	0	66.4	33.6
3	75	0	25	100	0
4	50	50	0	39.7	60.3
5	50	25	25	56.9	43.1
6	50	0	50	100	0
7	25	75	0	18.0	82.0
8	25	50	25	24.8	75.2
9	25	25	50	39.7	60.2
10	25	0	75	100	0
11	0	100	0	0	100
12	0	75	25	0	100
13	0	50	50	0	100
14	0	25	75	0	100

hence, different weight fractions are made for experiments. As shown in Fig. 4(b), for the model bale produced with just two HDPE sheets, the volume fractions of HDPE  $\phi_p$ , PVC  $\phi_f$  and air  $\phi_{air}$  are 50%, 0%, and 50%, respectively. By adding an additional PVC sheet into model bale, the volume fractions of PVC  $\phi_f$  and air  $\phi_{air}$  changes to 25%. In this study, seven different bales are made for investigating the relationships between mixture density and total mass, as well as between mixture permittivity and voltage output. Their volume fractions, mixture densities, and mixture permittivity are shown in Table II. These relationships are established as prior knowledge for the measurement. Fourteen different bales are prepared to evaluate the performance of the proposed method, and the volume fractions of HDPE, PVC, and air, along with the weight fractions of HDPE and PVC, are shown in Table III.

The sensor structure can be optimized and adjusted to accommodate the size of the HDPE bales. In this study, bales with a side length of 80 mm are used as experimental samples. After optimization, the parameters  $A$ ,  $B$ ,  $W$ , and  $L$  in the transmitter and receiver units are set to 93, 85, 3, and 1 mm, respectively, as these values provide the sensor with

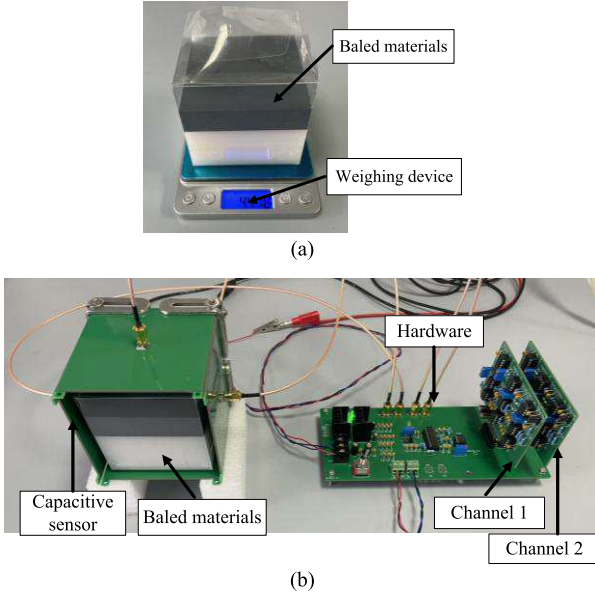


Fig. 5. (a) Weighing device. (b) Capacitive sensor.

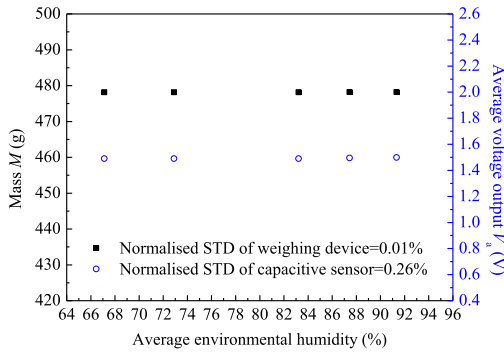


Fig. 6. Sensor outputs under different average environmental humidity.

high sensitivity and a satisfactory sensitivity distribution [26]. The transmitter units and the receiver units are fabricated on printed circuit boards (PCBs) with thickness  $t$  of 1.6 mm, and the capacitive sensor is formed. The sensing system comprising a weighing device and a capacitive sensor is shown in Fig. 5. The weighing device as shown in Fig. 5(a) obtains the mass information of the bales, which are directly related to the mixture density. The capacitive sensor as shown in Fig. 5(b) measures the bales using two measurement channels. Channel 1 is the capacitive sensor output from the bottom and top transceiver units, while channel 2 from left and right transceiver units. The voltage outputs of the sensor reflect the capacitance of the bale measured from two different directions, which closely related to the mixture permittivity. A data acquisition device is applied to sample the two-channel outputs of the sensor.

#### IV. RESULTS AND DISCUSSION

##### A. Sensor Outputs

The output characteristics of the weighing device and the capacitive sensor under different conditions were investigated. Considering that HDPE bales may be exposed to environments

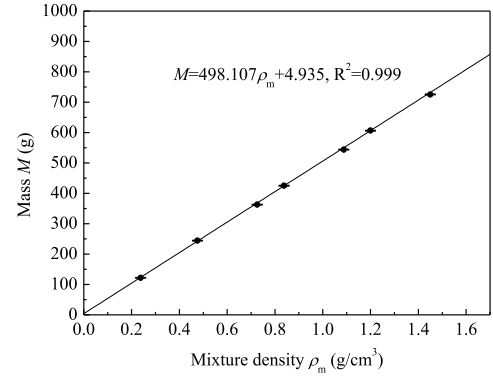


Fig. 7. Relationship between calculated mixture density and measured mass by the weighing device.

with varying humidity, we studied the effect of environmental humidity on sensor outputs. The HDPE bale was tested over five different days under different humidity conditions. Each day, the bale was exposed to the environment for eight hours. During this period, nine humidity values were collected at one-hour intervals, and the average humidity was subsequently calculated. The outputs of the weighing device and the capacitive sensor for the bale were then recorded providing the sensor outputs and corresponding average humidity for each day. The outputs  $M$  of the weighing device and the averaged two-channel outputs  $V_a$  of the capacitive sensor corresponding to different average environmental humidity are shown in Fig. 6. The outputs of the weighing device were similar under different humidity conditions, with normalized standard deviation (STD) of 0.01%. Similarly, the capacitive sensor also showed small normalized STD (0.26%) under different humidity conditions. This can be attributed to the bale having an extremely low water absorption rate. The results indicate that the influence of environmental humidity on the measurements can be considered negligible.

The output characteristics of the weighing device and the capacitive sensor under different bale types and material distributions were also investigated. The bales used are listed in Table II. Since the bale has three pairs of opposite faces, we define them as follows: bottom face, top face, left face, right face, front face, and back face. We aligned the bottom face, left face, and back face with the surface of the weighing device and the T1 electrode of capacitive sensor, resulting in three typical relative positions between the bale and the sensor. These relative positions lead to different nonuniform distributions of material. For each relative position, the output of weighing device and two-channel outputs of the capacitive sensor were measured.

Fig. 7 shows the relationship between the average of measured mass at three different relative positions and the corresponding mixture density  $\rho_m$ , which is calculated using (5). The error bars represent the STD calculated from these three measurements. This linear relationship indicates that the sensor output exhibits a high and consistent sensitivity to changes in the mixture density of bale. The variations in  $M$  are very small, indicating good measurement repeatability and low measurement uncertainty.

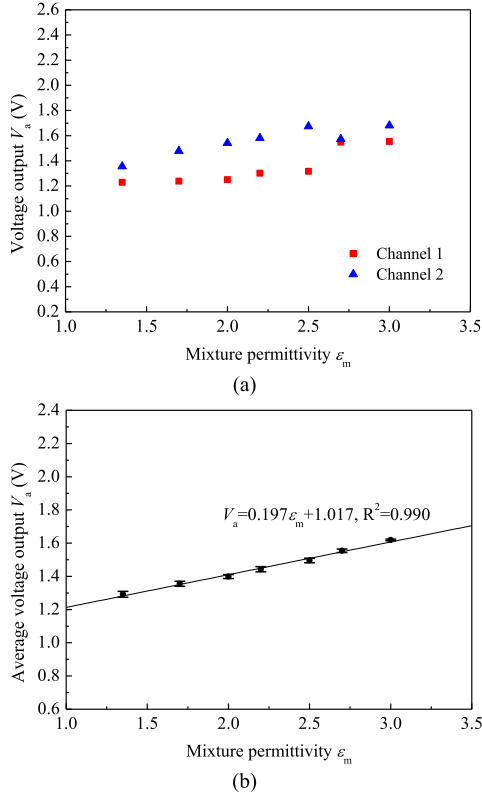


Fig. 8. (a) Two-channel voltage outputs of the capacitive sensor for bales with different mixture permittivity. (b) Relationships between the mixture permittivity and averaged voltage output of the capacitive sensor.

For the capacitive sensor, the corresponding sensor outputs from channels 1 and 2 for bales with different mixture permittivity are shown in Fig. 8(a). It can be seen that the voltage outputs of channels 1 and 2 are different because of the nonuniform distribution of materials between the two pairs of transceiver units. The output of a single channel is not able to represent the mixture permittivity due to the nonuniform distribution of materials in bales. Therefore, the average of the outputs from two channels is used to reduce the effect caused by material distribution. For each relative position, the voltage values from the two channels were averaged, and the average voltage output  $V_a$  was then obtained by averaging the results from the three measurements. The error bars represent the STD calculated from these three measurements. The averaged voltage output  $V_a$  along with the calculated mixture permittivity and the error bars are presented in Fig. 8(b). It can be seen that the average voltage output  $V_a$  exhibits a nearly linear relationship with the mixture permittivity  $\epsilon_m$ , which indicates that the sensor output exhibits a high and consistent sensitivity to changes in the mixture permittivity of bale. The variations in  $V_a$  is also small, which indicates that the averaged voltage output is relatively insensitive to the nonuniform distribution of the material, while also exhibiting good measurement repeatability and low measurement uncertainty.

### B. Establishment of Prior Knowledge

The bales in Table II were not only used to investigate the output characteristics of the sensors, but also provided data

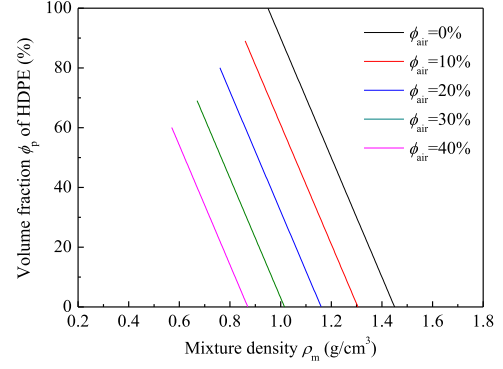


Fig. 9. Relationships between mixture density and volume fraction of HDPE when  $\phi_{air}$  are 0%, 10%, 20%, 30%, and 40%.

for establishing the prior knowledge of the weighing device and the capacitive sensor. To establish the prior knowledge about how the mixture density  $\rho_m$  depends on the measured mass  $M$  from the weighing device, a relationship between the calculated mixture density and the measured mass was fit based on Fig. 7. The corresponding equation is given as follows:

$$M = 498.107\rho_m + 4.935. \quad (12)$$

This prior knowledge will be used to determine the mixture density  $\rho_m$ , given the measured mass  $M$  of a bale to be tested.

To establish the prior knowledge about how the mixture permittivity  $\epsilon_m$  relates to the voltage output of the capacitive sensor, a relationship between the mixture permittivity and average voltage output of the capacitive sensor was fit based on Fig. 8(b). The corresponding equation is given as follows:

$$V_a = 0.197\epsilon_m + 1.017. \quad (13)$$

Based on (13), the mixture permittivity of the bale to be tested can be obtained from the voltage outputs.

### C. Development of Mathematical Model

In mathematical modeling, the specific expression for the volume fraction of HDPE needs to be determined based on (7) and (10). The densities and permittivity values of HDPE sheet, PVC sheet, and air are constant as summarized in Table I. By substituting these constants into (7) and (10), the volume fraction of HDPE can be expressed as follows:

$$\phi_p = \frac{-\rho_m - 1.449 \times \phi_{air} + 1.45}{0.5} \quad (14)$$

$$\phi_p = \frac{-\epsilon_m - 2 \times \phi_{air} + 3}{0.6}. \quad (15)$$

The volume fraction of air  $\phi_{air}$  is set to 0%, 10%, 20%, 30%, and 40% and the relationships between the mixture density  $\rho_m$  and the volume fraction  $\phi_p$  of HDPE under different values of  $\phi_{air}$  are plotted as shown in Fig. 9. For a given  $\phi_{air}$ , the mixture density decreases with the increase of the volume fraction of HDPE. This can be attributed to the fact that as the volume fraction of low-density HDPE increases, the volume fraction of high-density PVC decreases, resulting in a reduction in the overall mixture density. For a given  $\phi_p$ , the mixture density

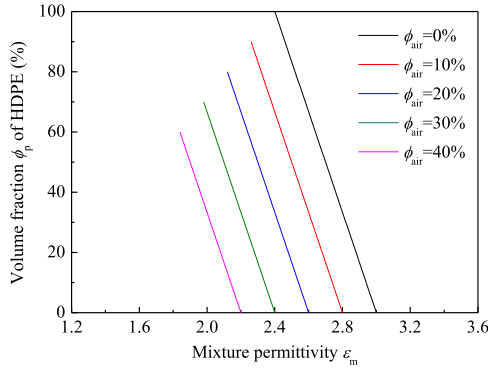


Fig. 10. Relationships between mixture permittivity and volume fraction of HDPE when  $\phi_{air}$  are 0%, 10%, 20%, 30%, and 40%.

decreases with the increase of the  $\phi_{air}$ . This can be attributed to the fact that the volume fraction of low-density air increases, the volume fraction of high-density PVC decreases, resulting in a reduction in the overall mixture density. When the  $\phi_{air}$  is unknown, it is difficult to determine the volume fraction of HDPE based on the mixture density.

Similarly, the relationships between the mixture permittivity  $\epsilon_m$  and the volume fraction  $\phi_p$  of HDPE under different air volume fraction conditions ( $\phi_{air} = 0\%$ , 10%, 20%, 30%, and 40%) are depicted in Fig. 10. For a given  $\phi_{air}$ , with the increase of the volume fraction of HDPE, the mixture permittivity decreases. This occurs because as the volume fraction of low-permittivity HDPE increases, the volume fraction of high-permittivity PVC decreases, resulting in a reduction in the overall mixture permittivity. For a given  $\phi_p$ , with the increase of the  $\phi_{air}$ , the mixture permittivity decreases. This is because as the volume fraction of low-permittivity air increases, the volume fraction of high-permittivity PVC decreases, leading to a reduction in the overall mixture permittivity. When the  $\phi_{air}$  is unknown, it is difficult to determine the volume fraction of HDPE based on the mixture density.

To obtain the  $\phi_{air}$ , (11) was defined, whose specific expression can be determined from (14) and (15)

$$\min \left| \frac{-\rho_m - 1.449 \times \phi_{air} + 1.45}{0.5} - \frac{-\epsilon_m - 2 \times \phi_{air} + 3}{0.6} \right| \quad (16)$$

s.t.  $0\% \leq \phi_{air} \leq 100\%$ .

By processing (16), the optimal  $\phi_{air}$  is determined and the HDPE volume fraction is subsequently calculated using (14).

#### D. Performance Evaluation

To evaluate the proposed method, the bales as shown in Table III are measured using the sensing system, respectively, to quantify the weight fractions of HDPE and PVC in these bales. By substituting the measured mass and the capacitive sensor outputs into (12) and (13), the mixture density, and permittivity of the bales are obtained. The derived mixture density and permittivity, along with possible values of  $\phi_{air}$  ( $0\% \leq \phi_{air} \leq 100\%$ ), are then applied to (16) to determine the minimum difference, as illustrated in Fig. 11. It can be seen that when the true value of  $\phi_{air}$  is 0%, the calculated

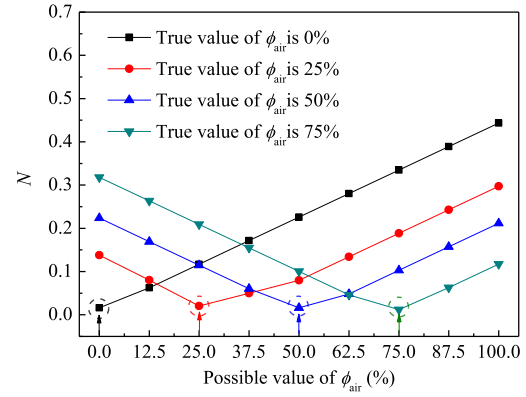


Fig. 11.  $N$  values with varying possible volume fractions of air when the true volume fraction of air is 0%, 25%, 50%, and 75%.

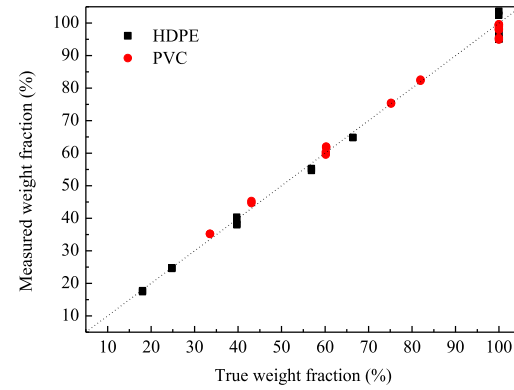


Fig. 12. Measured weight fractions of HDPE and PVC in comparison with their true values.

difference  $N$  reaches its minimum when the possible value of  $\phi_{air}$  is determined as 0%. As the possible values move further from the true value of 0%, the calculated  $N$  value increases. Therefore, by finding the minimum  $N$  value, the corresponding optimal value of  $\phi_{air}$  can be identified as the true value of  $\phi_{air}$ . For true values of  $\phi_{air}$  25%, 50%, and 75%, the same pattern is observed. When the possible values match the true values,  $N$  reaches its minimum. Thus, by searching for the minimum  $N$  value, the corresponding  $\phi_{air}$  value can be identified.

Once the true  $\phi_{air}$  is obtained, HDPE volume fraction  $\phi_p$  can be determined using (14) or (15). Equation (14) is adopted in this study because the weighing device provides more reliable and accurate measurements; then the weight fractions of HDPE and the contaminant PVC are calculated using (1)–(4). The measured weight fractions of HDPE and PVC in comparison with their true values are shown in Fig. 12. It can be seen that the measured values are very close to the true values. To quantify the measurement error, the relative errors of the measured weight fractions of HDPE and PVC are calculated and shown in Fig. 13. The calculated relative errors are small and are concentrated within a range of  $\pm 5\%$ . The results show that the proposed method can accurately measure the weight fractions of HDPE and PVC without being affected by the varying and unknown air volume fraction (i.e., uncertainty in packing density).



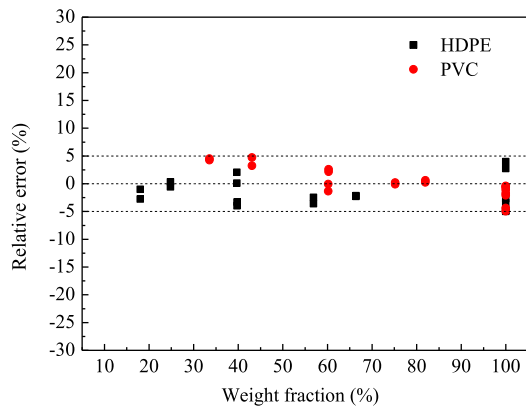


Fig. 13. Relative errors of the HDPE weight fraction and PVC weight fraction.

## V. CONCLUSION

In this study, a novel method combining a capacitive sensor system, a weighing device, and mathematical modeling is proposed for the first time to measure the weight fractions of an HDPE bale containing a single-known contaminant, independent of packing density. Experiments were carried out to evaluate the proposed method and the conclusions are as follows.

Relying solely on a traditional single-sensor approach, such as a weighing device or a capacitive sensor, is insufficient for measuring the weight fraction in HDPE bales with a contaminant under varying packing density conditions. This study utilizes a purpose-built capacitive sensor and a weighing device to simultaneously measure the bales. The experimental tests in this study found that the output of the capacitive sensor has a nearly linear relationship with the mixture permittivity, while the weighing device has a linear relationship with the mixture density. Based on their outputs, the mixture permittivity and the mixture density of the bale are acquired.

Through mathematical modeling, the relationships between the mixture permittivity, mixture density, and the volume fractions of individual components are established. It was found that variations in air volume fraction caused by packing density affect the measurement of the HDPE volume fraction, which in turn influences the measurement of the weight fraction. The novel mathematical model proposed in this study simultaneously incorporates both permittivity and density modeling, ultimately deriving the air volume fraction. Finally, the accurate measurement of the weight fractions in the HDPE bale is achieved. The relative errors of the measured weight fraction are within a range of  $\pm 5\%$ .

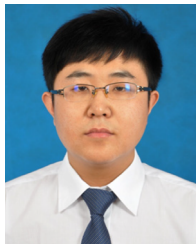
The proposed method can be extended to HDPE bales containing an unknown contaminant by employing identification approaches to determine the contaminant first. Our previous work [26] presented identification of baled materials using a two-channel capacitive sensor. Combining the capacitive sensor with a weighing device is expected to enhance the accuracy of material identification, even in scenarios where the bales exhibit the same permittivity but different HDPE-to-contaminant fractions, as the weighing device provides the additional density information of the bales. In the case of

HDPE bales containing multiple contaminants, determining the mixture permittivity and mixture density of the contaminants is crucial for applying the proposed method. In addition, the use of multisensor fusion technology along with machine learning techniques shows great potential to achieve both material identification and weight fraction measurement in more complex scenarios. Related work will be a focus of our future research.

## REFERENCES

- [1] Association of Plastic Recyclers. (Sep. 2022). *Model Bale Specifications: HDPE Colored Bottles*. Accessed: Oct. 2024. [Online]. Available: <https://assets.adspipe.com/m/5e7f9170277192ad/original/APR-Spec-on-HDPE-Color-Bales.pdf>
- [2] Association of Plastic Recyclers. (2023). *Model Bale Specifications: Mixed Small Rigid Plastics*. Accessed: Oct. 2024. [Online]. Available: <https://plasticsrecycling.org/wp-content/uploads/2024/09/APR-BaleSpec-MixedSmallRigidPlastic.pdf>
- [3] Environmental Services Association. (Sep. 2022). *Quality Standard Recycled Plastics*. Accessed: Oct. 2024. [Online]. Available: [https://www.recoup.org/wp-content/uploads/2023/09/ESA\\_Plastic\\_Standard.pdf](https://www.recoup.org/wp-content/uploads/2023/09/ESA_Plastic_Standard.pdf)
- [4] (Apr. 2014). *Sampling and Testing Guidance for Material Facilities*. Accessed: Oct. 2024. [Online]. Available: <https://www.wiserrecycling.co.uk/wp-content/uploads/2015/02/MF-Sampling-Guidance-April-2014.pdf>
- [5] R. Longo, S. Vanlanduit, and P. Guillaume, "Material properties identification using ultrasonic waves and laser Doppler vibrometer measurements: A multi-input multi-output approach," *Meas. Sci. Technol.*, vol. 24, no. 10, Oct. 2013, Art. no. 105206.
- [6] L. Harrision, M. Ravan, D. Tandel, K. Zhang, T. Patel, and R. K. Amineh, "Material identification using a microwave sensor array and machine learning," *Electronics*, vol. 9, no. 2, p. 288, Feb. 2020.
- [7] D. Jumanazarov, J. Koo, M. Busi, H. F. Poulsen, U. L. Olsen, and M. Iovea, "System-independent material classification through X-ray attenuation decomposition from spectral X-ray CT," *NDT E Int.*, vol. 116, Dec. 2020, Art. no. 102336.
- [8] O. Rozenstein, E. Puckrin, and J. Adamowski, "Development of a new approach based on midwave infrared spectroscopy for post-consumer black plastic waste sorting in the recycling industry," *Waste Manage.*, vol. 68, pp. 38–44, Oct. 2017.
- [9] C. Badini, O. Ostrovskaya, G. Bernagozzi, and A. Artusio, "Composition and workability of plastic fractions recovered from commingled waste discarded by a composting plant," *Polymers*, vol. 15, no. 7, p. 1690, Mar. 2023.
- [10] G. Bonifazi, M. D'Agostini, A. Dall'Ava, S. Serranti, and F. Turi-  
oni, "A new hyperspectral imaging based device for quality control in plastic recycling," *Proc. SPIE*, vol. 8774, pp. 365–377, May 2013.
- [11] Y. Zheng, J. Bai, J. Xu, X. Li, and Y. Zhang, "A discrimination model in waste plastics sorting using NIR hyperspectral imaging system," *Waste Manage.*, vol. 72, pp. 87–98, Feb. 2018.
- [12] M. Yunus, S. C. Mukhopadhyay, and G. S. Gupta, "A review of material properties estimation using eddy current testing and capacitor imaging," *Sens. Transducers*, vol. 100, pp. 92–115, Apr. 2009.
- [13] I. K. Ahmad, M. Mukhlisin, and H. Basri, "Application of capacitance proximity sensor for the identification of paper and plastic from recycling materials," *Res. J. Appl. Sci., Eng. Technol.*, vol. 12, no. 12, pp. 1221–1228, Jun. 2016.
- [14] I. K. Ahmad, S. N. Hidayah Harun, and M. R. Azmi, "An application of capacitance proximity sensor for identification of recyclable materials," *Jurnal Kejuruteraan*, vol. si1, no. 5, pp. 37–41, Nov. 2018.
- [15] M. Sun, S. Liu, J. Lei, and Z. Li, "Mass flow measurement of pneumatically conveyed solids using electrical capacitance tomography," *Meas. Sci. Technol.*, vol. 19, no. 4, Apr. 2008, Art. no. 045503.
- [16] Y. T. Wang, J. F. Yuan, G. Yang, and Y. F. Qiao, "Optimization design of capacitance sensor with helical shaped surface plates," *Adv. Mater. Res.*, vol. 508, pp. 92–95, Apr. 2012.
- [17] X. Wang, Y. Hu, H. Hu, and L. Li, "Evaluation of the performance of capacitance sensor for concentration measurement of gas/solid particles flow by coupled fields," *IEEE Sensors J.*, vol. 17, no. 12, pp. 3754–3764, Jun. 2017.

- [18] D. Wang, J. Sun, Y. Wang, G. Yang, Z. Zhu, and Z. Xie, "Eliminating the influence of moisture on solid concentration measurement in gas–solid flows using combined sensors," *IEEE Trans. Instrum. Meas.*, vol. 72, pp. 1–10, 2023.
- [19] K. Tang, H. Hu, L. Li, and X. Wang, "Sectional water fraction measurement for gas–water two-phase flow containing a conductive water phase utilizing capacitance sensor," *Meas. Sci. Technol.*, vol. 32, no. 5, May 2021, Art. no. 055104.
- [20] N. Li, M. Cao, X. Yu, J. Jia, and Y. Yang, "High sensitive capacitive sensing method for thickness detection of the water film on an insulation surface," *IEEE Access*, vol. 7, pp. 96384–96391, 2019.
- [21] J. Zheng and L. Peng, "An autoencoder-based image reconstruction for electrical capacitance tomography," *IEEE Sensors J.*, vol. 18, no. 13, pp. 5464–5474, Jul. 2018.
- [22] Q. Guo, M. Ye, W. Yang, and Z. Liu, "A machine learning approach for electrical capacitance tomography measurement of gas–solid fluidized beds," *AIChE J.*, vol. 65, no. 6, pp. 1–18, Jun. 2019.
- [23] A. Huang, Z. Cao, S. Sun, F. Lu, and L. Xu, "An agile electrical capacitance tomography system with improved frame rates," *IEEE Sensors J.*, vol. 19, no. 4, pp. 1416–1425, Feb. 2019.
- [24] Z. Liu, H. Wang, S. Sun, L. Xu, and W. Yang, "Investigation of wetting and drying process in a spout-fluid bed using acoustic sensor and electrical capacitance tomography," *Chem. Eng. Sci.*, vol. 281, Nov. 2023, Art. no. 119160.
- [25] X. Li et al., "A strategy to screen capacitances of adverse effects on image reconstruction for ECT sensors mounted outside thick pipe wall," *Measurement*, vol. 245, Mar. 2025, Art. no. 116645.
- [26] D. Wang, L. Wang, and Y. Yan, "Identification of baled materials through capacitive sensing and data driven modelling," *Meas., Sensors*, vol. 38, May 2025, Art. no. 101617.
- [27] W. Q. Yang, "Hardware design of electrical capacitance tomography systems," *Meas. Sci. Technol.*, vol. 7, no. 3, pp. 225–232, Mar. 1996.
- [28] M. J. D. Silva, E. Schleicher, and U. Hampel, "Capacitance wire-mesh sensor for fast measurement of phase fraction distributions," *Meas. Sci. Technol.*, vol. 18, no. 7, pp. 2245–2251, Jul. 2007.



**Dayang Wang** received the B.Sc. and M.Sc. degrees from Northeastern University, Shenyang, China, in 2012 and 2014, respectively, and the Ph.D. degree from Tianjin University, Tianjin, China, in 2020.

He joined Northeastern University, as a Lecturer, in 2020. He is currently a Research Associate in electronic engineering at the University of Kent, Canterbury, U.K. His research interests include industrial process measurement and instrumentation, microwave sensing technology, intelligent measurement systems, and information processing.



**Lijuan Wang** (Senior Member, IEEE) received the B.Eng. degree in computer science and technology from Qiqihar University, Qiqihar, Heilongjiang, China, in 2010, and the Ph.D. degree in measurement and automation from North China Electric Power University, Beijing, China, in 2014, and the Ph.D. degree in electronic engineering from the University of Kent, Canterbury, U.K., in 2017.

She is currently a Lecturer in electronic engineering with the School of Engineering, Mathematics and Physics, University of Kent. Her current research interests include material identification and measurement, multiphase flow measurement, condition monitoring of mechanical systems, smart sensors, and instrumentation systems.



**Yong Yan** (Fellow, IEEE) received the B.Eng. and M.Sc. degrees in instrumentation and control engineering from Tsinghua University, Beijing, China, in 1985 and 1988, respectively, and the Ph.D. degree in flow measurement and instrumentation from the University of Teesside, Middlesbrough, U.K., in 1992.

He was an Assistant Lecturer with Tsinghua University in 1988. In 1989, he joined as a Research Assistant with the University of Teesside. After a short period of Post-Doctoral Research, he was a Lecturer with the University of Teesside from 1993 to 1996. He was a Senior Lecturer, a Reader, and a Professor with the University of Greenwich, Chatham, U.K., from 1996 to 2004. He was a Professor of electronic instrumentation and the Director of research and innovation with the School of Engineering, University of Kent, Canterbury, U.K., from 2004 to 2024. He is currently a Lead Scientist and the Director of the International Research Center for Carbon Neutralization, Hangzhou International Innovation Institute, Beihang University, Hangzhou, China. His current research interests include multiphase flow measurement, combustion instrumentation, intelligent measurement, and condition monitoring.

Dr. Yan was elected as a fellow of the Royal Academy of Engineering in 2020. He was awarded the Gold Medal in 2020 by the IEEE TRANSACTIONS ON INSTRUMENTATION AND MEASUREMENT as the most published author of all time from the U.K.